CNGA2 Channels Mediate Adenosine-Induced Ca^{2+} Influx in Vascular Endothelial Cells

Kwong-Tai Cheng, Yuk-Ki Leung, Bing Shen, Yuk-Chi Kwok, Ching-On Wong, Hiu-Yee Kwan, Yu-Bun Man, Xin Ma, Yu Huang, Xiaoqiang Yao

Objectives—Adenosine is a cAMP-elevating vasodilator that induces both endothelium-dependent and -independent vasorelaxation. An increase in cytosolic Ca^{2+} ($[Ca^{2+}]_i$) is a crucial early signal in the endothelium-dependent relaxation elicited by adenosine. This study explored the molecular identity of channels that mediate adenosine-induced Ca^{2+} influx in vascular endothelial cells.

Methods and Results—Adenosine-induced Ca^{2+} influx was markedly reduced by L-*cis*-diltiazem and LY-83583, two selective inhibitors for cyclic nucleotide-gated (CNG) channels, in H5V endothelial cells and primary cultured bovine aortic endothelial cells (BAECs). The Ca^{2+} influx was also inhibited by 2 adenylyl cyclase inhibitors MDL-12330A and SQ-22536, and by 2 A_{2B} receptor inhibitors MRS-1754 and 8-SPT, but not by an A_{2A} receptor inhibitor SCH-58261 or a guanylyl cyclase inhibitor ODQ. Patch clamp experiments recorded an adenosine-induced current that could be inhibited by L-*cis*-diltiazem and LY-83583. A CNGA2-specific siRNA markedly decreased the Ca^{2+} influx and the cation current in H5V cells. Furthermore, L-*cis*-diltiazem inhibited the endothelial Ca^{2+} influx in mouse aortic strips, and it also reduced 5-*N*-ethylcarboxamidoadenosine (NECA, an A_2 adenosine receptor agonist)-induced vasorelaxation.

Conclusion—CNGA2 channels play a key role in adenosine-induced endothelial Ca^{2+} influx and vasorelaxation. It is likely that adenosine acts through A_{2B} receptors and adenylyl cyclases to stimulate CNGA2. (***Arterioscler Thromb Vasc Biol* 2008;28:913-918**)

Key words: CNGA2 channels ■ adenosine ■ cAMP ■ endothelial cells ■ Ca^{2+}

Adenosine is an endogenous nucleoside with potent vasodilatory capacities in many vascular beds.[1] Adenosine can be released from myocardium, endothelial cells, and skeletal muscles as a result of metabolism. The released adenosine then elicits vasorelaxation either by directly stimulating A_2-adenosine receptors in vascular smooth muscle cells, causing subsequent vasorelaxation,[1] or by indirectly acting on vascular endothelial cells, triggering endothelium-dependent vasorelaxation.[1–3]

Adenosine induces the endothelium-dependent vasorelaxation either via a Ca^{2+}-dependent mechanism[3–5] or a Ca^{2+}-independent mechanism.[2] In the former case, the adenosine-induced $[Ca^{2+}]_i$ rise stimulates endothelial cells to release vasorelaxants such as nitric oxide (NO)[3,6] and endothelium-derived hyperpolarizing factor (EDHF).[7] These vasodilators diffuse to nearby smooth muscle cells, causing vascular smooth muscle relaxation. At least in some arteries, this $[Ca^{2+}]_i$ rise is a prerequisite for adenosine-induced vasodilator release and vasorelaxation.[3–5] For example, in skeletal muscle arterioles, adenosine elicits an endothelial $[Ca^{2+}]_i$ rise,[3,5] and chelation of endothelial $[Ca^{2+}]_i$ with intraluminal perfusion of BAPTA-AM abolishes the adenosine-induced vasorelaxation, indicating an obligatory role of endothelial $[Ca^{2+}]_i$ in this relaxation.[3,5] In another study, it was found that adenosine induces NO release from rat aortic endothelium in situ, and this NO release requires Ca^{2+} influx.[4]

Virtually nothing is known about the molecular identity of channels that mediate adenosine-induced Ca^{2+} influx in endothelial cells. Multiple Ca^{2+}-permeable channels are expressed in vascular endothelial cells. These include TRP channels[8] and CNG channels.[9–12] CNG channels are activated by cAMP and cGMP,[13] the levels of which are elevated when endothelial cells are exposed to adenosine.[1,14,15] The activity of CNG channels can be inhibited by L-*cis*-diltiazem and LY-83583.[16,17] The L-*cis* isomer of diltiazem selectively blocks CNG channels, whereas the D-*cis*-isomer inhibits L-type Ca^{2+} channels.[16] Among 3 functional CNG isoforms (CNGA1-A3), CNGA2 has a much higher sensitivity to cAMP than other CNG isoforms.[13] This property makes CNGA2 a more likely downstream target for adenosine. Previously, most CNGA2-related studies were carried out in olfactory sensory neurons, where CNGA2 form heterotetramers with 2 modulatory subunits CNGA4 and CNGB1.[13] In the present study, we tested the hypothesis that CNG channels are involved in adenosine-induced Ca^{2+} influx in vascular endothelial cells. Our results demonstrated that CNG channels,

Original received May 18, 2007; final version accepted February 11, 2008.

From the Li Ka Shing Institute of Health Sciences and Department of Physiology, Faculty of Medicine, the Chinese University of Hong Kong, China.
Correspondence to Xiaoqiang Yao, PhD, Department of Physiology, The Chinese University of Hong Kong, Hong Kong, China. E-mail yao2068@cuhk.edu.hk

Arterioscler Thromb Vasc Biol **is available at http://atvb.ahajournals.org** **DOI: 10.1161/ATVBAHA.107.148338**

especially CNGA2, mediate the adenosine-induced Ca^{2+} influx in these cells, and that CNG channels may play an important role in endothelium-dependent vasorelaxation in response to A_2 adenosine receptor agonists.

Materials and Methods

Cell Culture and Ca^{2+} Dye Loading

H5V cells, which were derived from murine embryonic heart endothelium, and were grown in 90% DMEM and 10% FBS. Before experiments, the endothelial cells were loaded with 10 μmol/L Fluo-3/AM in a physiological saline solution (PSS) that contained in mmol/L: 140 NaCl, 5 KCl, 1 $CaCl_2$, 10 glucose, 5 Hepes, pH 7.4.

Vessel Preparation and Ca^{2+} Dye Loading

The animal study was conducted in conformity with the *Guide for animal Care and Use of Laboratory Animals* published by the US National Institute of Health. For $[Ca^{2+}]_i$ measurements, thoracic aorta from male C57 mice was cut into a small strip, and then mounted onto an experimental chamber with endothelial surface facing the objectives. The endothelial layer was then fluorescently loaded with 10 μmol/L Fluo-4/AM.

CNGA2-Specific siRNA and Transfection

The vector-based siRNA strategy was used. The CNGA2-specifc siRNA sequence was designed using Ambion siRNA Target Finder. A pair of inverted repeat sequences containing the 19-nt siRNA was then synthesized. The sequence for the strand 1 was 5′-TGGCAAAGATGACCACAGGTTCAAGAGACCTGTGGTCATCTTTGCCATTTTTT-3′, and that for strand 2 was 5′-AATTAAAAAATGGCAAAGATGACCACAGGTCTCTTGAACCTGTGGTCATCTTTGCCAGGCC-3′. The CNGA2-specific nucleotides are underlined. These 2 strands were annealed and then cloned into a self-constructed siRNA expression vector pcDU6C. H5V cells were stably transfected with the pcDU6C containing either the CNGA2-specific siRNA or a control siRNA with scrambled sequence.

Immunoblots

Briefly, whole-cell proteins were extracted. 100 μg proteins were loaded onto each lane and separated on a SDS/PAGE gel. Proteins were transferred to a polyvinylidene fluoride (PVDF) membrane, and blotted with the primary anti-CNGA2 (1:1000), anti-CNGA4 (2 μg/mL), or anti-A_{2B} receptor antibody (1:100). The bound antibodies were detected with horseradish peroxidase-conjugated secondary antibody.

$[Ca^{2+}]_i$ Measurements

Briefly, the experimental chambers containing either cultured endothelial cells or isolated aortic strips were placed on the stage of an inverted microscope (Olympus IX81), and the $[Ca^{2+}]_i$ fluorescence was measured using a FV1000 laser scanning confocal imaging system. Changes of $[Ca^{2+}]_i$ were displayed as a ratio of fluorescence relative to the fluorescence before the application of adenosine or 8-BrcAMP (F1/F0).

$[Ca^{2+}]_i$ rise was initiated by applying adenosine (100 μmol/L) to the cultured cells bathed in PSS. For aortic strips, the Fluo-4/AM-loaded vessel strips were bathed in a solution that contained in mmol/L: 118 NaCl, 4.7 KCl, 2.5 $CaCl_2$, 1.2 KH_2PO_4, 25.2 $NaHCO_3$, 11.1 glucose, pH 7.4, bubbled with 95% O_2-5% CO_2. When appropriate, inhibitors were added 10 minutes before the initiation of adenosine-induced Ca^{2+} influx. A slightly higher concentration of L-*cis*-diltiazem was used for the mouse aortic strips to overcome the relative poor penetration of the chemical in this tissue (100 μmol/L for tissue versus 50 μmol/L for H5V cells).

Electrophysiology

Whole-cell current was recorded using an EPC9 patch clamp amplifier (HEKA) in voltage-clamp mode. Patch pipette contained in mmol/L: 145 Na^+-glutamate, 5 CsCl, 5 EGTA, 5 Hepes, pH 7.4. Bath solution contained in mmol/L: 145 Na^+-glutamate, 5 Hepes, 10 glucose, pH 7.4. Adenosine (100 μmol/L) was applied to the cells held at −80 mV. Instantaneous *I-V* relationships were obtained by applying an ascending ramp protocol from −100 mV to +100 mV for 500 ms before and after adenosine application. L-*cis*-diltiazem and LY-83583 were added 10 minutes before adenosine application.

Arterial Tension Measurement

Segments of aorta were dissected from male C57 mice and mounted in a myograph. Isometric tension was measured. Cumulative concentration–response relationships for the relaxant effect of NECA were determined in aortic rings after steady contraction with 11-deoxy prostaglandin (PG) $F_{2\alpha}$. The concentration of 11-deoxy $PGF_{2\alpha}$ varied from 60 to 300 nmol/L to achieve similar degree of constriction in different arteries. If needed, L-*cis*-diltiazem (100 μmol/L), L-NAME (100 μmol/L), or charybdotoxin (50 nmol/L) plus apamin (50 nmol/L) was added 30 minutes before NECA application. In some arterial rings, the endothelial layer was mechanically removed.

For detailed experimental procedures, please see the supplemental materials (available online at http://atvb.ahajournals.org).

Results

Role of CNG Channels in Adenosine-Induced Ca^{2+} Influx in H5V Cells

Application of adenosine (100 μmol/L) elicited a $[Ca^{2+}]_i$ rise in H5V cells bathed in PSS (Figure 1A). This $[Ca^{2+}]_i$ rise was attributable to Ca^{2+} influx, because (1) removal of extracellular Ca^{2+} abolished the $[Ca^{2+}]_i$ rise; (2) adenosine also induced Mn^{2+} influx as will be described later. We then explored the possible involvement of CNG channels in this Ca^{2+} influx. L-*cis*-diltiazem, a highly selective inhibitor for CNG channels,[16] caused a dose-dependent inhibition on this Ca^{2+} influx (supplemental Figure I). L-*cis*-diltiazem at 50 μmol/L markedly reduced the percentage of cells displaying adenosine-induced Ca^{2+} influx (Figure 1D). This agent also decreased the magnitude of $[Ca^{2+}]_i$ rise among the responding cells (Figure 1B and 1E). Another CNG channel inhibitor LY-83583[17] (20 μmol/L) had similar effect to that of L-*cis*-diltiazem (Figure 1C through 1E).

Because both L-*cis-diltiazem* and LY-83583 inhibit multiple CNG isoforms, they cannot be used to differentiate specific CNG isoform(s) involved. Thus, siRNA strategy was used to study the possible involvement of CNGA2 in H5V cells. CNGA2 was chosen as the possible target based on its high sensitivity to cAMP[13] and its expression in vascular endothelial cells.[9,11,12] In immunoblot experiments, a CNGA2-specific antibody recognized a protein band with molecular size of ≈80 kDa, which correlates well with that of mouse CNGA2 in Genbank (NM_007724).[18] Stable expression of a CNGA2-specific siRNA reduced the CNGA2 protein level by 80±2% (n=5) (Figure 2A and 2C). In contrast, stable expression of a control siRNA had no effect on the CNGA2 protein level (Figure 2A). The effect of CNGA2-siRNA was specific to CNGA2, because it had no effect on the expression of another CNG isoform CNGA4 (≈66 kDa, NM_001033317) (Figure 2B and 2C). Functionally, the CNGA2-specific siRNA not only reduced the percentage of cells displaying adenosine-induced Ca^{2+} influx (Figure 2F), but also decreased the magnitude of adenosine-induced $[Ca^{2+}]_i$ rise among the responding cells (Figure 2E and 2G). In contrast, the control siRNA had no effect on this Ca^{2+} influx (Figure 2F and 2G). Mn^{2+} influx studies were performed to verify the results of

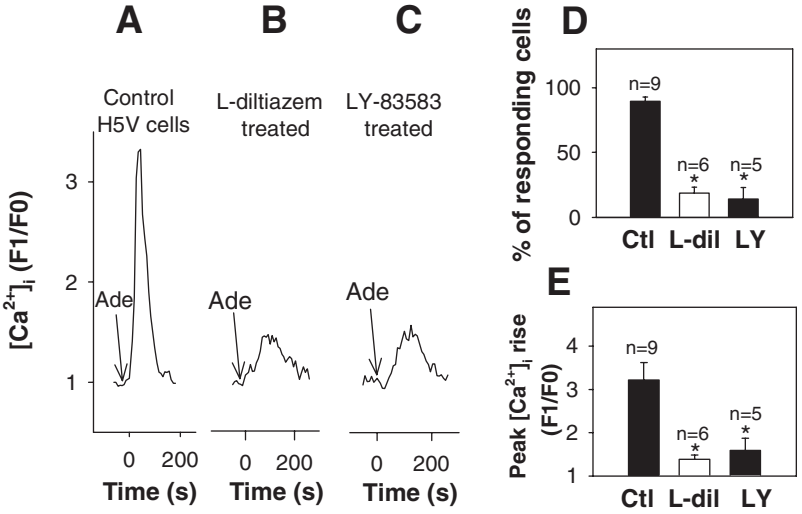

Figure 1. Effect of CNG channel inhibitors on adenosine-induced Ca^{2+} influx in H5V cells. A-C, Representative traces of adenosine (100 μmol/L)-induced Ca^{2+} influx in control (A), L-*cis*-diltiazem (50 μmol/L)-treated (B, a responding cell), and LY-83583 (20 μmol/L)-treated cells (C, a responding cell). D and E, Summary of data showing the effect of chemicals on the percentage of cells displaying adenosine-induced Ca^{2+} influx (D) and on the peak $[Ca^{2+}]_i$ rise among the responding cells (E). Ctl indicates control; L-dil, L-*cis*-diltiazem; LY, LY-83853. Mean±SEM (n=5 to 9 experiments, 15 to 40 cells per experiment). *$P<0.01$ compared to the control.

Ca^{2+} influx studies. The adenosine-induced Mn^{2+} influx was also reduced by the CNGA2-specific siRNA but not by the control siRNA (supplemental Figure II). Taken together, these data strongly suggest that CNGA2 is the main channel responsible for adenosine-induced Ca^{2+} influx in H5V cells.

Role of CNG Channels in Adenosine-Induced Inward Current in H5V Cells

Whole cell patch clamp was used to verify the involvement of CNGA2 in the adenosine-induced responses. Application of adenosine (100 μmol/L) elicited an inward current in cells clamped at −80 mV (Figure 3A). Because the adenosine-induced inward current was transient (Figure 3A), an ascending voltage-ramp protocol was applied from −100 mV to +100 mV for 500 ms to obtain instantaneous *I-V* relationships before and after the adenosine application (Figure 3A and 3B). The results show that adenosine could stimulate the outward current at positive membrane potential and enhance the inward current at negative membrane potential (Figure 3B and 3G). More importantly, treatment with L-*cis*-diltiazem (50 μmol/L; Figure 3C, 3D, and 3H) and CNGA2-specific siRNA (Figure 3E, 3F, and 3H) diminished the adenosine-induced current in H5V cells. In contrast, the control siRNA had no effect (Figure 3H). These data agree with the results from the fluorescent Ca^{2+} influx experiments and support a role of CNGA2 channels in the adenosine-induced current.

Note that, even in the presence of L-*cis*-diltiazem, there are some background cation current in H5V cells (Figure 3D). It is likely that this background current might be contributed by other cation channels such as TRP channels.[8]

Involvement of Adenylyl Cyclases and A_{2B} Receptors

Adenosine may act on A_2 receptors to stimulate adenylyl cyclases, resulting in an increased cytosolic cAMP level.[1,15] Adenosine may also stimulate guanylyl cyclases, thus elevating cytosolic cGMP level.[14] Both cAMP and cGMP can activate CNGA2 channels. To test possible involvement of adenylyl cyclases and guanylyl cyclases, we used SQ-22536 and MDL-12330A, both of which inhibit adenylyl cyclases, and ODQ, which inhibits guanylyl cyclases. SQ-22536 caused a dose-dependent inhibition on adenosine-induced Ca^{2+} influx (supplemental Figure I). SQ-22536 at 300 μmol/L and MDL-12330A at 10 μmol/L drastically reduced the percentage of cells displaying adenosine-induced Ca^{2+} influx (11±4% [n=9] for SQ-22536-treated, 14±6% [n=7] for MDL-12330A-treated versus 88±3% [n=13] for the control cells), and they also markedly decreased the magnitude of $[Ca^{2+}]_i$ rise among the responding cells (F1/F0 of 1.6±0.1 [n=9] for SQ-22536-treated, 1.5±0.2 [n=7] for MDL-12330A-treated versus 3.2±0.3 [n=13] for the control cells). In contrast, ODQ treatment (50 μmol/L) had no effect

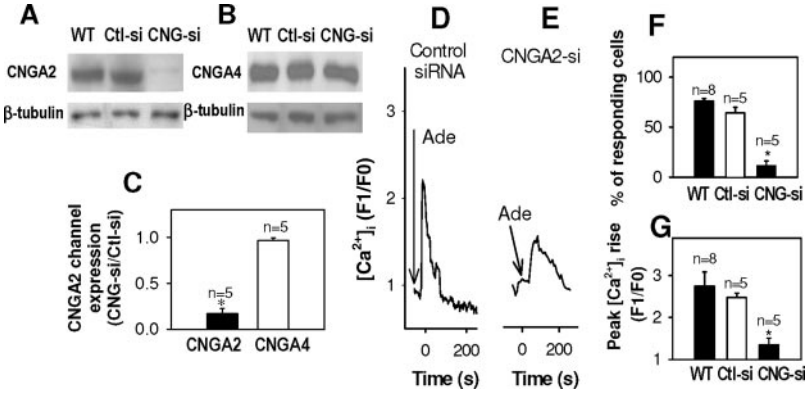

Figure 2. Effect of CNGA2-specific siRNA on adenosine-induced Ca^{2+} influx in H5V cells. A-C, Representative images (A, B) and summary (C) of immunoblot experiments. D and E, Representative traces showing adenosine (100 μmol/L)-induced Ca^{2+} influx in control-siRNA-transfected (D) and CNGA2-siRNA-transfected cells (E, a responding cell). F and G, Summary of data showing the effect of CNGA2-specific siRNA on the percentage of cells displaying adenosine-induced Ca^{2+} influx (F) and on the peak $[Ca^{2+}]_i$ rise among the responding cells (G). WT indicates wild-type; Ctl-si, control siRNA-transfected; CNG-si, CNGA2-siRNA-transfected. Mean±SEM (n=5 to 8 experiments, 15 to 40 cells per experiment). *$P<0.01$ compared to the control siRNA-transfected cells.

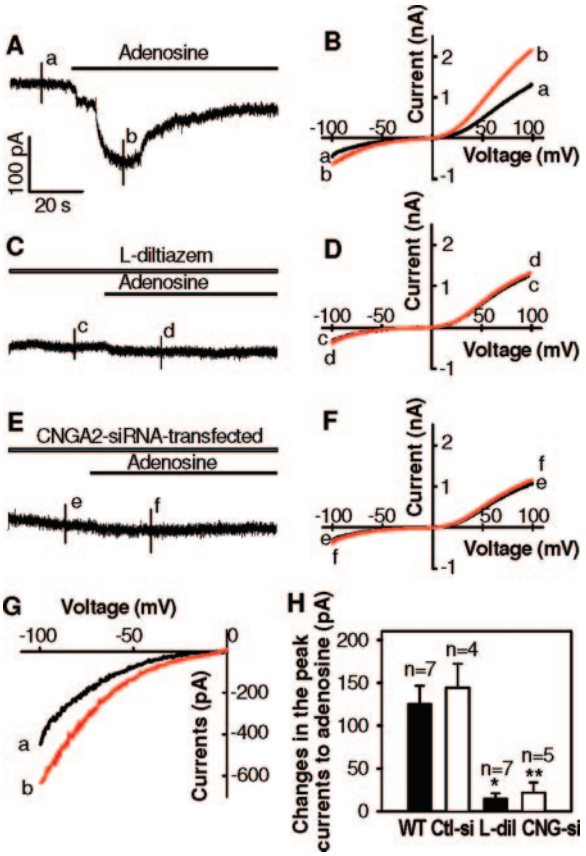

Figure 3. Effect of L-*cis*-diltiazem and the CNGA2-specific siRNA on adenosine-elicited current in H5V cells. A, C, and E, Representative inward current traces in control (A), L-*cis*-diltiazem (50 μmol/L)-treated (C), and CNGA2-siRNA-transfected cells (E) clamped at −80 mV. B, D and F, Instantaneous *I-V* relationships at the time point *a-f*. G, Part of B ranging from −100 mV to 0 mV. H, Summary of the data showing the effect of different treatments on adenosine-induced peak inward current for cells clamped at −80 mV. Mean±SEM (n=4 to 7 experiments). *$P<0.01$ compared to wild-type (WT) cells. **$P<0.01$ compared to control-siRNA-transfected (Ctl-si) cells.

either on the percentage of cells displaying adenosine-induced Ca^{2+} influx (87±3% [n=6] versus 88±3% [n=13] for the control cells) or on the magnitude of $[Ca^{2+}]_i$ rise among the responding cells (F1/F0 of 2.8±0.4 [n=6] versus 3.2±0.3 [n=13] for the control cells). These data suggest an involvement of adenylyl cyclases but not guanylyl cyclases.

Adenosine may act either on A_{2A} or A_{2B} receptors to stimulate adenylyl cyclases.[15] An A_{2A}-specific inhibitor SCH-58261,[15] an A_{2B}-specific inhibitor MRS-1754,[15] and a relatively A_1- and A_{2B}-selective inhibitor 8-SPT[19] were used to differentiate the involvement of A_{2A} and A_{2B}. Both MRS-1754 and 8-SPT caused a dose-dependent inhibition on adenosine-induced Ca^{2+} influx (supplemental Figure I). MRS-1754 at 50 nmol/L and 8-SPT at 1 μmol/L (a concentration that may only inhibit A_{2B} and A_1 receptors)[19] drastically reduced the percentage of responding cells (41±7% [n=4] for MRS-1754-treated, 3±1% [n=4] for 8-SPT-treated versus 88±3% [n=13] for the control cells), and they also markedly decreased the magnitude of $[Ca^{2+}]_i$ rise among the responding cells (F1/F0 of 2.0±0.1 [n=4] for MRS-1754-treated, 1.6±0.1 [n=4] for 8-SPT-treated versus 3.2±0.3 [n=13] for the control cells). In contrast, SCH-58261 had no effect (supplemental Figure I). The expression of A_{2B} receptors in H5V cells was also confirmed by RT-polymerase chain reaction (PCR) and immunoblot experiments (supplemental Figure III). These data suggest an involvement of A_{2B} but not A_{2A} receptors.

Role of CNGA2 in 8-BrcAMP-Induced Ca^{2+} Influx and Cation Current in H5V Cells

Exogenous cAMP was used to further study the regulatory role of cAMP in CNGA2-mediated Ca^{2+} influx and cation current. Application of membrane-permeant 8-Br-cAMP (100 μmol/L) induced a $[Ca^{2+}]_i$ rise (supplemental Figure IVA and IVB) and a cation current in H5V cells (supplemental Figure IVC through VE). Both the $[Ca^{2+}]_i$ rise and the cation current were inhibited by the CNGA2-specific siRNA, L-*cis*-diltiazem and LY83583 (supplemental Figure IV).

Role of CNG Channels in the Primary Cultured BAECs

H5V is a cell line. There is a concern that endothelial phenotype may change during prolonged cell culture and cell passage conditions. Thus, we used the primary cultured BAECs to verify the above findings. Similar to H5V cells, adenosine induced a $[Ca^{2+}]_i$ rise in BAECs (supplemental Figure V), and this $[Ca^{2+}]_i$ rise was abolished in the presence of *L-cis*-diltiazem and LY-83583 (supplemental Figure V). Patch clamp experiments also showed that the adenosine-stimulated current was inhibited by L-*cis*-diltiazem and LY-83583 in BAECs (supplemental Figure VI).

Role of CNG Channels in Adenosine-Induced Endothelial Ca^{2+} Influx in Mice Aorta

About one fourth of the endothelial cells in mice aortic strips were found to display spontaneous $[Ca^{2+}]_i$ transients, some cells with a single $[Ca^{2+}]_i$ transient and others with repetitive $[Ca^{2+}]_i$ oscillations. The rest (three fourths) cells were quiescent. Application of adenosine (100 μmol/L) elicited a transient $[Ca^{2+}]_i$ rise in 12±2% (n=8) of endothelial cells, which were previously quiescent (Figure 4A through 4C). Some cells responded with a single $[Ca^{2+}]_i$ transient whereas others responded with repetitive $[Ca^{2+}]_i$ transients. This adenosine-induced endothelial $[Ca^{2+}]_i$ rise was almost completely abolished in aortic strips that were pretreated with L-*cis*-diltiazem (100 μmol/L) for 10 minutes (Figure 4C). We also tested LY-83583 (20 μmol/L). However, LY-83583 itself greatly facilitated the spread of Ca^{2+} signals to neighboring cells presumably because of its action on gap junctions (n=4), thus this agent was not used further. Because of the difficulty in determining the exact cell boundary of individual endothelial cells in mouse aortic strips with our confocal microscope system, which significantly hampered our ability of accurately estimating the change in $[Ca^{2+}]_i$, we did not attempt to analyze the magnitude of $[Ca^{2+}]_i$ rise. Instead, only the effect of L-*cis*-diltiazem on the percentage of responding cells was compared (Figure 4C).

One may query about the physiological importance of these adenosine-induced $[Ca^{2+}]_i$ transients, because relatively low percentage of endothelial cells (12±2%, n=8) in isolated aortic strips responded to adenosine. However, note that the endothelial cells in situ are known to display heterogeneity,

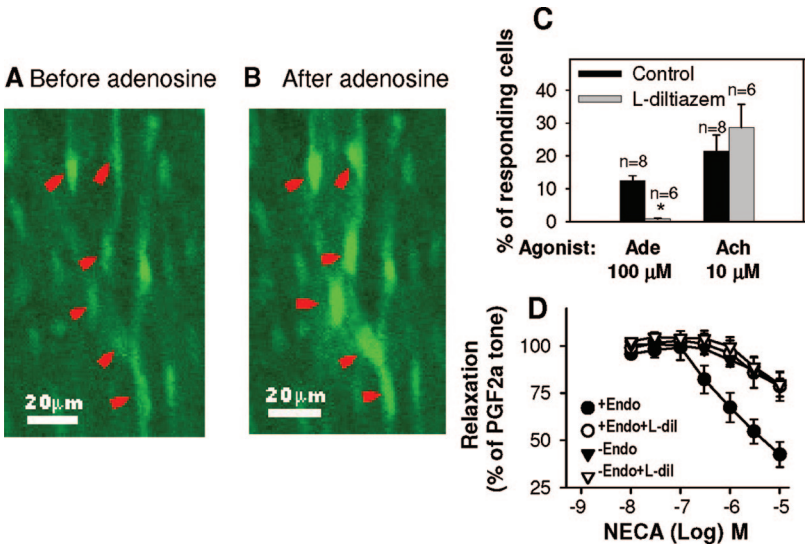

Figure 4. Effect of L-*cis*-diltiazem on adenosine- and acetylcholine-induced endothelial $[Ca^{2+}]_i$ rises within mouse aortic strips (A-C), and on NECA-induced vasorelaxation in mouse aortic segments (D). A and B, Representative endothelium fluorescence images before (A) and after (B) 100 μmol/L adenosine. Red arrows point to the adenosine-responding cells. C and D, Summary of data showing the effect of L-*cis*-diltiazem (L-dil, 100 μmol/L) on the percentage of cells displaying adenosine (Ade, 100 μmol/L)- and acetylcholine (Ach, 1 μmol/L)-induced Ca^{2+} rise (C), and on NECA-induced relaxation (D). +Endo indicates endothelium-intact; -Endo, endothelium-denuded. Mean±SEM (n=6 to 10 experiments). *$P<0.01$ as compared to the control.

with different population of cells responding to different agonists.[20] Therefore, it is expected that only certain percentage of cells can respond to adenosine. For comparison, in our experiment, a well-recognized vasoactive agonist acetylcholine (1 μmol/L) elicited $[Ca^{2+}]_i$ transients in 21±5% (n=8) of the endothelial cells in aortic strips (Figure 4C), and furthermore this acetylcholine-induced $[Ca^{2+}]_i$ rise is insensitive to L-*cis*-diltiazem (100 μmol/L) (Figure 4C).

Role of CNG Channels in A_2 Adenosine Receptor-Mediated Vasorelaxation

We further examined the functional role of CNG channels in adenosine receptor-mediated vasorelaxation. In agreement with the results from other groups,[21] NECA, a selective A_2 adenosine receptor agonist, induced concentration-dependent vasorelaxation in mouse aortic segments preconstricted with 11-deoxy PG $F_{2\alpha}$ (Figure 4D, supplemental Figure VIIA). The relaxation was mostly endothelium-dependent, because removal of the endothelium greatly reduced NECA-induced relaxation (Figure 4D). Importantly, L-*cis*-diltiazem (100 μmol/L) markedly inhibited the vasorelaxation to NECA in normal (endothelium-intact) aortic rings (Figure 4D, supplemental Figure VII), but it had no effect on the residual small relaxation to NECA in endothelium-denuded aortic rings (Figure 4D). These data suggest that CNG channels play a key role in the endothelium-dependent relaxation induced by NECA. We also explored the vasodilator(s) involved in NECA-induced relaxation. L-NAME (100 μmol/L) reduced the NECA-induced relaxation in endothelium-intact aortic rings to a level similar to that of endothelium-denuded rings (supplemental Figure VIIC). Furthermore, combined application of charybdotoxin (50 nmol/L) and apamin (50 nmol/L), a treatment considered to be a hallmark of EDHF response,[7] had no effect on the NECA-induced relaxation (supplemental Figure VIIC). These results suggest that the NECA-induced vasorelaxation is mediated by NO but not EDHF.

Note that the adenosine-induced $[Ca^{2+}]_i$ rise and cation current were transient (Figures 1A and 3A), whereas the NECA-induced vasorelaxation lasted much longer (supplemental Figure VIIA). This is reasonable, because the vasorelaxation involves the Ca^{2+}-NO–protein kinase G signaling pathway and the protein kinase G–mediated protein phosphorylation,[22] which has a much long-lasting effect.

Discussion

Adenosine is a key metabolite involved in metabolic hyperemia in many vascular beds including coronary circulation, cerebral circulation, and skeletal muscle circulation.[1] The roles of adenosine in vasculature are most prominent during hypoxia, ischemia, and reactive hyperemia.[1] One important action of adenosine is to induce endothelium-dependent vasorelaxation.[1–4] It is previously shown that, at least in some arteries, such as skeletal muscle arteries, a rise in $[Ca^{2+}]_i$ is required for the endothelium-dependent vasorelaxation in response to adenosine.[3–5] In the present study, we explored the possible role of CNG channels in adenosine-induced Ca^{2+} influx in vascular endothelial cells. Our results show that the adenosine-induced Ca^{2+} influx was markedly reduced by CNG-specific inhibitors L-*cis*-diltiazem and LY-83583 in H5V cells and in the primary cultured BAECs. Whole cell patch clamp recorded an adenosine-induced current that was sensitive to L-*cis*-diltiazem in both cell types. Furthermore, a CNGA2-specific siRNA almost completely abolished the adenosine-induced Ca^{2+} influx current in H5V cells. Moreover, L-*cis*-diltiazem inhibited adenosine-induced endothelial $[Ca^{2+}]_i$ rise in isolated mouse aortic strips, and it also markedly reduced the endothelium-dependent vasorelaxation to NECA, an A_2 adenosine receptor agonist. It was also found that the NECA-induced vasorelaxation was mediated by NO but not by EDHF. These data provide compelling evidence that CNG channels, CNGA2 in particular, play a key role in adenosine-induced endothelial Ca^{2+} influx and subsequent vasorelaxation.

CNG channels are Ca^{2+}-permeable nonselective cation channels activated by cyclic nucleotides cAMP and cGMP.[13] It is previously documented that adenosine may increase cAMP and cGMP by stimulating adenylyl cyclases and guanylyl cyclases in endothelial cells.[1,14,15] In the present study, adenosine-induced endothelial Ca^{2+} influx was drastically reduced by adenylyl cyclase inhibitors MDL-12330A and SQ-22536, but not affected by guanylyl cyclase inhibitor ODQ. Exogenous application of membrane-permeant 8-BrcAMP also induced Ca^{2+} influx. These data suggest that

cAMP but not cGMP is the second messenger that links adenosine to CNGA2 activation. Adenosine may interact with 4 G protein–coupled receptors, A_1, A_{2A}, A_{2B}, and A_3. Stimulation of A_1 and A_3 receptors inactivates adenylyl cyclases, resulting in a decreased cAMP level, whereas stimulation of A_{2A} and A_{2B} receptors activates adenylyl cyclases, leading to an increased cAMP level.[15] In the present study, the adenosine-induced Ca^{2+} influx was inhibited by MRS-1754 and 8-SPT but not by SCH-58261, suggesting an involvement of A_{2B} but not A_{2A} receptors. Taken together, it appears that adenosine binds to A_{2B} receptors, causing activation of adenylyl cyclases, which elevate cytosolic cAMP level, leading to an increased activity of CNGA2 channels.

In 2 published functional studies, Zhang et al[12] proposed that CNGA2 contributes to the store-operated Ca^{2+} influx induced by thapsigargin in pulmonary artery endothelial cells, whereas Wu et al[11] suggested that CNGA2 mainly allows Na^+ entry, resulting in membrane depolarization, which reduces the driving force for Ca^{2+} entry. In the present study, we showed for the first time that CNGA2 mediates adenosine-induced endothelial Ca^{2+} entry and vasorelaxation. This finding fits well with a unique property of CNGA2, ie, its higher sensitivity to cAMP than other CNG isoforms.[13] Note that vascular endothelial cells in vivo are also the targets of several other physiologically important cAMP-elevating agents including calcitonin gene-related peptide,[23] adrenomedullin,[23] and adrenaline (through β-receptors).[24] In future, it will be interesting to explore whether CNG channels also participate in the vasorelaxation in response to other cAMP-elevating agents.

Previous studies also found the expression of 2 other CNG isoforms, CNGA1 and CNGA4, in vascular endothelial cells.[9–12] However, CNGA1 is unlikely to be involved in the adenosine-induced responses, because CNGA1 is not sensitive to cAMP.[13] CNGA4 is not a functional subunit and cannot form a functional channel by itself. The role of CNGA4, if any, is to modulate the function of native endothelial CNG channels. There is a possibility that CNGA4 may form heteromeric channels with CNGA2 in endothelial cells as in the case for olfactory neurons.[13] Further experiments are needed to clarify whether such an association between CNGA2 and CNGA4 indeed exists in endothelial cells.

In conclusion, we demonstrated that CNG channels, especially CNGA2, play a key role in adenosine-induced endothelial Ca^{2+} influx and subsequent vasorelaxation. It is likely that adenosine acts through A_{2B} receptors and adenylyl cyclases to stimulate CNGA2 in endothelial cells.

Sources of Funding

This study was supported by Hong Kong Research Grant Council (CUHK4526/06m and Li Ka Shing Institute of Health Sciences.

Disclosures

None.

References

1. Tabrizchi R, Bedi S. Pharmacology of adenosine receptors in the vasculature. *Pharmacol Ther*. 2001;91:133–147.
2. Wyatt AW, Steinert JR, Wheeler-Jones CP, Morgan AJ, Sugden D, Pearson JD, Sobrevia L, Mann GE. Early activation of the p42/p44MAPK pathway mediates adenosine-induced nitric oxide production in human endothelial cells: a novel calcium-insensitive mechanism. *FASEB J*. 2002;16:1584–1594.
3. Duza T, Sarelius IH. Conducted dilations initiated by purines in arterioles are endothelium dependent and require endothelial Ca^{2+}. *Am J Physiol Heart Circ Physiol*. 2003;285:H26–H37.
4. Ray CJ, Marshall JM. The cellular mechanisms by which adenosine evokes release of nitric oxide from rat aortic endothelium. *J Physiol*. 2006;570:85–96.
5. Duza T, Sarelius IH. Increase in endothelial cell Ca^{2+} in response to mouse cremaster muscle contraction. *J Physiol*. 2004;555:459–469.
6. Govers R, Rabelink TJ. Cellular regulation of endothelial nitric oxide synthase. *Am J Physiol Renal Physiol*. 2001;280:F193–F206.
7. Busse R, Edwards G, Feletou M, Fleming I, Vanhoutte PM, Weston AH. EDHF: bringing the concepts together. *Trends Pharmacol Sci*. 2002;23:374–380.
8. Yao X, Garland CJ. Recent developments in vascular endothelial cell transient receptor potential channels. *Circ Res*. 2005;97:853–863.
9. Cheng KT, Chan FL, Huang Y, Chan WY, Yao X. Expression of olfactory-type cyclic nucleotide-gated channel (CNGA2) in vascular tissues. *Histochem Cell Biol*. 2003;120:475–481.
10. Yao X, Leung PS, Kwan HY, Wong TP, Fong MW. Rod-type cyclic nucleotide-gated cation channel is expressed in vascular endothelium and vascular smooth muscle cells. *Cardiovasc Res*. 1999;41:282–290.
11. Wu S, Moore TM, Brough GH, Whitt SR, Chinkers M, Li M, Stevens T. Cyclic nucleotide-gated channels mediate membrane depolarization following activation of store-operated calcium entry in endothelial cells. *J Biol Chem*. 2002;275:18887–18896.
12. Zhang J, Xia SL, Block ER, Patel JM. NO upregulation of a cyclic nucleotide-gated channel contributes to calcium elevation in endothelial cells. *Am J Physiol Cell Physiol*. 2002;283:C1080–C1089.
13. Kaupp UB, Seifert R. Cyclic nucleotide-gated ion channels. *Physiol Rev*. 2002;82:768–824.
14. Olanrewaju HA, Mustafa SJ. Adenosine A_{2A} and A_{2B} receptors mediated nitric oxide production in coronary artery endothelial cells. *Gen Phamacol*. 2000;35:171–177.
15. Fredholm BB, IJzerman AP, Jacobson KA, Klotz KN, Linden J. International Union of Pharmacology. XXV. Nomenclature and classification of adenosine receptors. *Pharmacol Rev*. 2001;53:527–552.
16. Finn JT, Grunwald ME, Yau KW. Cyclic nucleotide-gated ion channels: an extended family with diverse functions. *Ann Rev Physiol*. 1996;58:395–426.
17. Leinders-Zufall T, Rand MN, Shepherd GM, Greer CA, Zufall F. Calcium entry through cyclic nucleotide-gated channels in individual cilia of olfactory receptor cells: spatiotemporal dynamics. *J Neurosci*. 1997;17:4136–4148.
18. Bonigk W, Bradley J, Muller F, Sesti F, Boekhoff I, Ronnett GV, Kaupp UB, Frings S. The native rat olfactory cyclic nucleotide-gated channel is composed of three distinct subunits. *J Neurosci*. 1999;19:5332–5347.
19. Gao Z, Li BS, Day YJ, Linden J. A3 adenosine receptor activation triggers phosphorylation of protein kinase B and protects rat basophilic leukemia 2H3 mast cells from apoptosis. *Mol Pharmacol*. 2001;59:76–82.
20. Huang TY, Chu TF, Chen HI, Jen CJ. Heterogeneity of $[Ca^{2+}]_i$ signaling in intact rat aortic endothelium. *FASEB J*. 2000;14:797–804.
21. Fahim M, Hussain T, Mustafa SJ. Relaxation of rat aorta by adenosine in diabetes with and without hypertension: role of endothelium. *Eur J Pharmacol*. 2001;412:51–59.
22. Lincoln TM, Dey N, Sellak H. cGMP-dependent protein kinase signaling mechanisms in smooth muscle: from the regulation of tone to gene expression. *J Appl Physiol*. 2001;91:1421–1430.
23. Brain SD, Grant AD. Vascular actions of calcitonin gene-related peptide and adrenomedullin. *Physiol Rev*. 2003;84:903–934.
24. Guimaraes S, Moura D. Vascular adrenoceptors: an update. *Pharmacol Rev*. 2001;53:319–356.

Supplemental methods

Cell culture and Ca^{2+} dye loading

H5V cells, which were derived from murine embryonic heart endothelium transformed with polyoma middle-sized T antigen, were a generous gift from Dr. Vecchi A, Italy (Garlanda C et al., 1994). H5V cells were grown in 90% DMEM and 10% FBS with 100 U/ml penicillin and 100 μg/ml streptomycin. The primary cultured BAECs were isolated from bovine aorta. Briefly, bovine aortic segments were cut open longitudinally. The intima layer was peeled off with the help of scalpel blade, and the segments were then digested with 0.1% collagenase in PBS (in mmol/L: 140 NaCl, 3 KCl, 25 Tris, pH 7.4) for 15 min at 37°C under vigorous shaking. Dissociated cells were centrifuged, re-suspended, and then grown in a culture medium that contained 90% RPMI-1640 and 10% FBS with 100 U/ml penicillin and 100 μg/ml streptomycin. Only the cells from the first four passages were used for experiments.

Before experiments, the endothelial cells were grown on circular discs, and then loaded with 10 μmol/L Fluo-3/AM and 0.02% pluronic F-127 for 1 hour in dark at 37°C in a physiological saline solution (PSS) that contained in mmol/L: 140 NaCl, 5 KCl, 1 $CaCl_2$, 10 glucose, 5 Hepes, pH 7.4. The cells were then mounted onto an experimental chamber.

Vessel preparation and Ca^{2+} dye loading

Male C57 mice (6–8 week old) were killed by carbon dioxide and the thoracic aorta was immediately dissected. The aorta was cut into small strips (3 mm width x 5 mm long) and pinned onto a base plate. The plate was mounted onto an experimental chamber with endothelial surface facing the objectives. The distance between the endothelial surface and the cover-slip at the bottom of the chamber was ~2 mm with the Krebs solution freely passed between them. The Krebs solution had the following composition in mmol/L: 118 NaCl, 4.7 KCl, 2.5 $CaCl_2$, 1.2 $MgSO_4$, 1.2 KH_2PO_4, 25.2 $NaHCO_3$, 11.1 glucose, pH 7.4, and bubbled with 95% O_2-5% CO_2. The endothelial layer of aortic strips was fluorescently labeled by incubating with 10 μmol/L Fluo-4/AM and 0.02% pluronic F-127 in the Krebs solution for 10 min at room temperature.

$[Ca^{2+}]_i$ measurements

$[Ca^{2+}]_i$ measurements were performed as described elsewhere (Kwan HY et al., 2004). Briefly, the experimental chambers mounted either with cultured endothelial cells or isolated

aortic strips were placed on the stage of an inverted microscope (Oymplus IX81), and the $[Ca^{2+}]_i$ fluorescence was measured using the FV1000 laser scanning confocal imaging system at room temperature. The excitation wavelength was at 488 nm and the fluorescence signals were collected using a 515 nm long pass emission filter. Data analysis was performed with FV1000 software. Changes of $[Ca^{2+}]_i$ were displayed as a ratio of fluorescence relative to the fluorescence before the application of adenosine or 8-BrcAMP (F1/F0).

A $[Ca^{2+}]_i$ rise was initiated by applying adenosine (100 μmol/L) to the cultured cells bathed in PSS. This $[Ca^{2+}]_i$ rise was due to Ca^{2+} influx, because 1) removal of extracellular Ca^{2+} abolished the $[Ca^{2+}]_i$ rise; 2) adenosine was able to induce Mn^{2+} influx; 3) in the presence of adenosine (100 μmol/L), application of extracellular Ca2+ (1 mmol/L) could also induce a $[Ca^{2+}]_i$ rise. Note that these H5V cells had normal ability of store Ca^{2+} releasing, because several well-known store Ca^{2+}-releasing agonists, including bradykinin, ATP and acetylcholine, could elicit a $[Ca^{2+}]_i$ rise in the absence of extracellular Ca^{2+} (data not shown). Unless described otherwise, H5V cells and the primary cultured BAECs were pretreated with 4 μmol/L thapsigargin for 30 min in PSS to deplete intracellular Ca^{2+} stores. This procedure eliminated the possible contribution of Ca^{2+} influx-induced intracellular Ca^{2+} release towards the overall $[Ca^{2+}]_i$ rise (Leung PC et al., 2006). For aortic strips, no thapsigargin pretreatment was performed and the vessel strips were bathed in a solution that contained in mmol/L: 118 NaCl, 4.7 KCl, 2.5 $CaCl_2$, 1.2 KH_2PO_4, 25.2 $NaHCO_3$, 11.1 glucose, pH 7.4, bubbled with 95% O_2-5% CO_2. When needed, inhibitors were added 10 minutes before the application of adenosine. For the primary cultured BAECs and the mouse aortic strips, we used a slightly high concentration of L-*cis*-diltiazem (100 μmol/L) to overcome the relative poor penetration of the chemical in these cells/tissues.

Measurement of Mn^{2+} influx

Mn^{2+} influx was measured using the FV1000 laser scanning confocal imaging system at room temperature. H5V cells were loaded with 10 μmol/L Fluo-3/AM for 1 hour in dark at 37°C with 0.02% Pluronic F127 in culture medium. Cells were bathed in PSS. Immediately before the adenosine (100 μM) challenge, the cells were transferred to Mn^{2+}-PSS, which contained in mmol/L: 140 NaCl, 5 KCl, 1 $MnCl_2$, 10 glucose, 5 Hepes, pH 7.4. Adenosine-induced Mn^{2+} influx resulted in a quenching in Fluo-3 fluorescence. The magnitude of Mn^{2+} influx was displayed as a decrease in fluorescence intensity in percentage.

Electrophysiology

Whole-cell current was recorded using an EPC9 patch clamp amplifier (HEKA) in voltage-clamp mode, controlled by Pulse/PulseFit 8.8 software. Patch pipette (resistance 5–6 MΩ) solution contained in mmol/L: 145 Na^+-glutamate, 5 CsCl, 5 EGTA, 5 Hepes, pH 7.4 adjusted with TEA-OH. Bath solution contained in mmol/L: 145 Na^+-glutamate, 5 Hepes, 10 glucose, pH 7.4 adjusted with TEA-OH. 100 μmol/L adenosine or 100 μmol/L 8-BrcAMP was applied to the cells held at -80 mV. Instantaneous *I-V* relationships were obtained by applying an ascending ramp protocol from -100 mV to +100 mV for 500 ms before and after adenosine/8-BrcAMP application. All currents were sampled at 50 kHz and filtered at 5 kHz, and the data were analyzed with PulseFit. Electrophysiological experiments were performed at room temperature. L-*cis*-diltiazem and LY-83583 were added 10 min before adenosine application.

siRNA and transfection

We followed a strategy developed by Brummelkamp *et al.* (2002) to allow H5V cells to stably express siRNA using a vector-based inverted repeat sequence forming a hairpin structure *in vivo*. A 19-nt siRNA sequence against mouse CNGA2 gene was designed using Ambion siRNA Target Finder. A pair of inverted repeat sequences containing the 19-nt siRNA was then synthesized. The sequence for the strand 1 was 5'-TGGCAAAGATGACCACAGGTTCAAGAGACCTGTGGTCATCTTTGCCATTTTTT-3', and that for strand 2 was 5'-AATTAAAAAATGGCAAAGATGACCACAGGTCTCTTGAACCTGTGGTCATCTTTGCCAGGCC-3'. The CNGA2-specific nucleotides are underlined. This sequence is specific to CNGA2 only, and it does not cross-react with other CNG isoforms. These two strands were annealed and then cloned into a self-constructed siRNA expression vector pcDU6C (Leung PC et al., 2006). pcDU6C contains a U6 RNA polymerase III promoter and a blasticidin resistance gene. The insertion of siRNA sequence was verified by DNA sequencing using ABI autosequencer (Perkin Elmer).

H5V cells were transfected with pcDU6C containing either CNGA2-specific siRNA or a control siRNA with scrambled sequence. The transfection was carried out using Lipofectamine 2000. Under the selection pressure of 2 μg/ml blasticidin, the stable cell lines expressing either the CNGA2-specific siRNA or the control siRNA were established in ~10 days.

Immunoblots

Immunoblots were performed as described elsewhere (Kwan HY et al., 2004). Briefly, whole-cell lysates were extracted with protein extraction buffer, which contained in mmol/L: 50 Tris-HCl, 150 NaCl, 50 NaF, 2 EDTA, and 1% Nonidet P-40, 0.1% SDS, 0.5% sodium deoxycholate, pH 7.5, with addition of the protease inhibitor cocktail tablets (Roche). Protein concentrations were determined by Bradford assay. 100 μg proteins were loaded onto each lane and separated on either an 8% SDS/PAGE gel (for detecting CNGA2 and CNGA4) or a 15% SDS/PAGE gel (for detecting A_{2B} receptors) after boiled in the SDS loading buffer. Proteins were transferred to a PVDF membrane, and the membrane was then immersed in a blocking solution containing 5% non-fat milk and 0.1% Tween 20 in PBS for 1 hour at room temperature with constant shaking. The incubation with the primary antibody against CNGA2 (1:1000), CNGA4 (2 μg/ml), or A_{2B} receptors (1:100) was carried out overnight at 4°C in PBS containing 5% non-fat milk and 0.1% Tween 20. Immunodetection was accomplished with horseradish peroxidase-conjugated secondary antibody, followed by ECL™ Plus western blotting detection system. Immunoblots with anti-β-tubulin antibody were used to confirm that an equal amount of proteins was loaded onto each lane. The intensity of the bands was analyzed by FluorChem 8000 imaging system.

Reverse transcription polymerase chain reaction

Total RNA was extracted from H5V cells using Trizol reagents and then treated with DNase I. The RNA was reverse-transcribed into first-strand cDNA with oligo(dT)12-18 primers using SuperScript II Reverse Transcriptase. The PCR primers specific for A_{2B} receptors was designed based on a previous publication (Yan D et al., 2006). The sequences of the primers were 5'-CAAGTGGGTGATGAATGTGG-3' and 5'-TTTCCGGAATCAATTCAAGC-3'. PCR reactions of 50 μl included 2 μl of the first-strand cDNA, 2 units of *Taq* DNA polymerase, 50 mmol/L KCl, 1.5 mmol/L $MgCl_2$, 0.2 mmol/L dNTPs, 0.6 μmol/L primers, 20 mmol/L Tris-HCl, pH 8.4. Thirty-five cycles (95°C for 30 sec, 55°C for 30 sec, 72°C for 30 sec) were performed with a PTC-200 PCR machine (MJ Research). The amplified 449-bp PCR product was resolved in a 2% agarose gel and stained with ethidium bromide.

Arterial tension measurement

The thoracic aorta was dissected from male C57 mice and cut into rings of 3 mm in length. The vessels were mounted in a myograph (model 610M, DMT, Denmark) under a normalized tension as previously described (Dora KA et al., 2001). Before commencing the experiments, all artery segments were allowed to equilibrate for about 60 min at 37^{o}C in Krebs solution bubbled with 95% O_2 and 5% CO_2. After equilibration, the aortic rings were challenged with KCl (60 mmol/L) until constant and reproducible contractions were achieved. Such preparations were used in the subsequent experiments

The aortic rings were preconstricted with 11-deoxy prostaglandin $F_{2\alpha}$ to achieve sustained contractions. The concentration of 11-deoxy prostaglandin $F_{2\alpha}$ varied from 60 to 300 nmol/L in order to achieve similar degree of constriction in different arteries. NECA was then added in a cumulative fashion to the bath to obtain the concentration–response curves. L-*cis*-diltiazem (100 μmol/L), L-NAME (100 μmol/L), or charybdotoxin (50 nmol/L) plus apamin (50 nmol/L) was added 30 min before NECA application. L-*cis*-diltiazem did not cause a significant change in contraction of aortic rings to 11-deoxy prostaglandin $F_{2\alpha}$. The relaxation response to NECA was expressed as % of 11-deoxy prostaglandin $F_{2\alpha}$-induced tone. In some experiments, the endothelial layer was mechanically disrupted with a small piece of plastic tubing. Endothelium integrity or functional removal was verified by the presence or absence, respectively, of the relaxant response (over 80% relaxation) to 1 μmol/L acetylcholine at the start of each experiment. All tension experiments were performed at 37^{o}C in Krebs solution.

Materials

Fluo-3/AM, Fluo-4/AM, and pluronic F-127 were obtained from Molecular Probes Inc. The primary antibodies against CNGA2, CNGA4, and A_{2B} receptors were from Alpha-Diagnostic Int., USA. ECL^{TM} Plus western blotting detection system was from Amersham Pharmacia. Protease inhibitor cocktail tablets were from Roche. L-*cis*-diltiazem was from Biomol, USA. RPMI-1640, DMEM, Trizol, FBS, blasticidin, and lipofectamine 2000, and *Taq* DNA polymerase were from Invitrogen. Thapsigargin and ODQ (1H-[1,2,4]oxadiazolo[4,3-a]quinoxalin-1-one) were from Tocris. 11-deoxy prostaglandin $F_{2\alpha}$ was from Cayman Chemicals. LY-83583, MDL-12330A, SQ-22536, and MRS-1754 [*N*-(4-cyanophenyl)-2-[4-(2,3,6,7-tetrahydro-2,6-dioxo-1,3-dipropyl-1*H*-purin-8-yl)-phenoxy]acetamide] were from Calbiochem. Adenosine, SCH-58261, NECA (5-*N*-ethylcarboxamidoadenosine), 8-SPT (8-(p-sulfophenyl)theophylline), L-NAME (N-nitro-L-arginine methyl ester), apamin,

charybdotoxin, nonidet P-40, sodium deoxycholate, SDS, EDTA, EGTA, Hepes, and Tris-HCl were from Sigma.

Supplemental results

Dose dependent inhibition by a panel of pharmacological agents on adenosine-induced Ca^{2+} influx in H5V cells

We used different concentrations of inhibitors to examine their effects on adenosine-induced Ca^{2+} influx in H5V cells. These inhibitors include a CNG-selective inhibitor L-*cis*-diltiazem, an adenylyl cyclase inhibitor SQ-22536, an A_{2B} adenosine receptor inhibitor MRS-1754, and an A_{2A} adenosine receptor inhibitor SCH-58261. In addition, we also used 8-SPT, an inhibitor that is relatively selective for A_{2B} and A_1 adenosine receptors. All these inhibitors except SCH-58261 reduced the percentage of cells displaying the adenosine-induced Ca^{2+} influx in a dose-dependent manner (Supplemental figure IA). These inhibitors (except SCH-58261) also caused a dose-dependent inhibition on the magnitude of $[Ca^{2+}]_i$ rise among the responding cells (Supplemental figure IB). These results suggest an important role of CNG channels, adenylyl cyclases, and A_{2B} adenosine receptors in adenosine-induced Ca^{2+} influx in H5V cells.

Effect of CNGA2-specific siRNA on adenosine-induced Mn^{2+} influx in H5V cells

We also performed Mg^{2+} quenching study to confirm the functional role of CNGA2 in adenosine-induced Ca^{2+} influx. Mn^{2+} is known to be a good substitute for Ca^{2+} in defining Ca^{2+} influx pathways. Because there is no intracellular Mn^{2+} store, the quenching reflects Mn^{2+} influx through the plasma membrane alone. Application of adenosine (100 μmol/L) caused Mn^{2+} influx, resulting in a decrease in fluo-3 fluorescence intensity (Supplemental figure IIA). In agreement with the data from Ca^{2+} influx studies, CNGA2-specific siRNA reduced the percentage of cells displaying adenosine-induced Mn^{2+} quenching (Supplemental figure IID), and it also decreased the magnitude of Mn^{2+} quenching among the responding cells (Supplemental figure IIC, and IIE). In contrast, the control siRNA had no effect on adenosine-induced Mn^{2+} quenching (Supplemental figure IIB, IID, and IIE).

Inhibitory properties of L-*cis*-diltiazem on cation current in H5V cells

In most experiments, cells were pre-incubated with L-*cis*-diltiazem to demonstrate its effect (Figure 3). In another series of experiments, L-*cis*-diltiazem (50 μmol/L) was directly applied

to cells, and it inhibited the cation current in both adenosine-stimulated and unstimulated H5V cells (data not shown). An inhibitory effect of L-*cis*-diltiazem in unstimulated H5V cells suggests the existence of basal CNG channel activity in native endothelial cells. These data are consistent with the notion that CNGA2 has spontaneous activity in the absence of cyclic nucleotides (Kleene SJ, 2000).

Detection of A_{2B} adenosine receptors in H5V cells by RT-PCR and immunoblot

RT-PCR was used to determine the existence of A_{2B} receptor mRNA in H5V cells. The PCR primers were designed based on a previous publication (Yang D et al., 2006). The RT-PCR amplified a cDNA fragment with expected molecular size of ~450 bp (Supplemental figure IIIA). Two negative controls were used. In the first negative control, the same experimental procedures were used except that the step of reverse transcription was omitted. In the second negative control, PCR was performed in the absence of cDNA template. No amplified product could be detected in both controls (Supplemental figure IIIA).

Immunoblots were used to further confirm the expression of A_{2B} receptor proteins in H5V cells. In immunoblot experiments, an antibody against A_{2B} adenosine receptors recognized a protein band with molecular size of ~35 kDa (Supplemental figure IIIB), which correlates well with that of mouse A_{2B} receptors in Genbank (NM_007413).

Role of CNGA2 in 8-BrcAMP-induced Ca^{2+} influx and cation current in H5V cells

Exogenous cAMP was used to further study the regulatory role of cAMP in CNGA2-mediated Ca^{2+} influx. Membrane-permeant 8-Br-cAMP (100 μmol/L) induced a $[Ca^{2+}]_i$ rise (Supplemental figure IVA, IVB). This $[Ca^{2+}]_i$ rise was due to Ca^{2+} influx, because 8-BrcAMP failed to evoke the $[Ca^{2+}]_i$ rise in H5V cells bathed in $0Ca^{2+}$-PSS (data not shown). The 8-BrcAMP-induced $[Ca^{2+}]_i$ rise was almost completely abolished by the CNGA2-specific siRNA and L-*cis*-diltiazem (50 μmol/L) (Supplemental figure IVB). In contrast, the control siRNA had no effect on the 8-BrcAMP-$[Ca^{2+}]_i$ rise (Supplemental figure IVB).

Patch clamp experiments show that 8-BrcAMP (100 μmol/L) elicited an inward cation current for cells clamped at -80 mV (Supplemental figure IVC). Instantaneous *I-V* relationship was determined before and after 8-BrcAMP application (Supplemental figure IVD). The results show that the 8-BrcAMP-induced cation current was inhibited by the CNGA2-specific siRNA, L-*cis*-diltiazem (50 μmol/L) and LY-83583 (20 μmol/L).

(Supplemental figure IVE). Taken together, it is clear that 8-BrcAMP can increase Ca^{2+} influx by activating CNGA2 in H5V cells.

Role of CNG channels in the primary cultured BAECs

H5V is a cell line. There is a concern that endothelial phenotype may change during a prolonged cell culture and cell passage conditions. Thus, we used the primary cultured BAECs to verify the above findings obtained from H5V cells. Similar to H5V cells, adenosine challenge (100 μmol/L) induced a $[Ca^{2+}]_i$ rise in BAECs (Supplemental figure VA), and this $[Ca^{2+}]_i$ rise was abolished in the presence of L-*cis*-diltazem (100 μmol/L) or LY-83583 (20 μmol/L) (Supplemental figure VB-VD). After L-*cis*-diltazem or LY-83583 treatment, almost none of cells could still respond to adenosine.

Patch clamp experiments show that adenosine (100 μmol/L) elicited an inward cation current for cells clamped at -80 mV (Supplemental figure VIA). Instantaneous *I-V* relationship was determined before and after adenosine application (Supplemental figure VIA-VID). The results show that the adenosine-induced cation current was inhibited by L-*cis*-diltiazem (100 μmol/L) and LY-83583 (20 μmol/L) in BAECs (Supplemental figure VIC-VIE).

Role of CNG channels in A_2 adenosine receptor-mediated vasorelaxation

NECA, a selective A_2 adenosine receptor agonist, induced concentration-dependent vasorelaxation in mouse aortic segments preconstricted with 11-deoxy prostaglandin $F_{2\alpha}$ (Figure 4D, Supplemental figure VIIA). Importantly, L-*cis*-diltiazem (100 μmol/L) markedly inhibited the vasorelaxation to NECA in normal endothelium-intact aortic rings (Figure 4D, Supplemental figure VIIB). These data suggest that CNG channels play a key role in the endothelium-dependent relaxation induced by NECA. We also explored the vasodilator(s) involved in NECA-induced relaxation. L-NAME (100 μmol/L) reduced the NECA-induced relaxation in endothelium-intact aortic rings to a level similar to that of endothelium-denuded rings (Figure 4D, Supplemental figure VIIC). Furthermore, combined application of charybdotoxin (50 nmol/L) and apamin (50 nmol/L), had no effect on the NECA-induced

relaxation (Supplemental figure VIIC). These results suggest that the NECA-induced vasorelaxation is mediated by NO but not EDHF.

Supplemental figure I

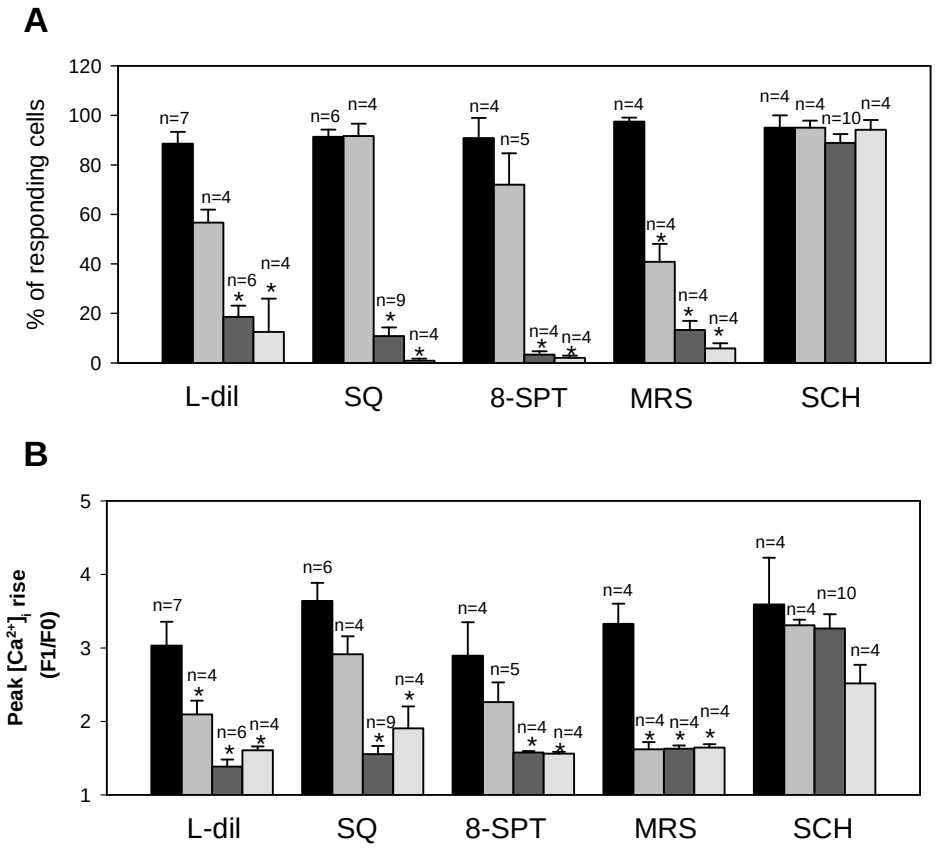

Supplemental figure I. Dose dependent inhibition by a panel of pharmacological agents on adenosine-induced Ca^{2+} influx in H5V cells. A and B, summary of data showing the effect of chemicals on the percentage of cells displaying adenosine-induced Ca^{2+} influx (A) and on the peak $[Ca^{2+}]_i$ rise among the responding cells (B). For each inhibitor, four concentrations were used. The results were displayed in four columns from left to right in an order of ascending concentration. L-dil, L-*cis*-diltiazem (0, 10 μmol/L, 50 μmol/L, 500 μmol/L); SQ: SQ-22536 (0, 30 μmol/L, 300 μmol/L, 3 mmol/L); 8-SPT (0, 100 nmol/L, 1 μmol/L, 10 μmol/L); MRS: MRS-1754 (0, 50 nmol/L, 500 nmol/L , 5 μmol/L); SCH: SCH-58261 (0, 10 nmol/L, 100 nmol/L, 1 μmol/L). Mean±SEM (*n*=4-10 independent experiments, 15 to 40 cells per experiment). **P*<0.01 as compared to controls (without inhibitor).

Supplemental figure II

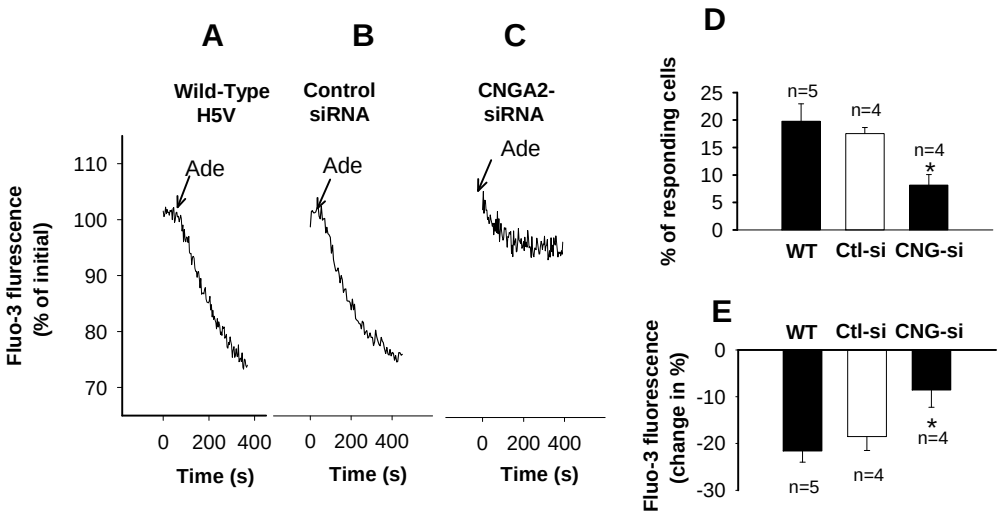

Supplemental figure II. Effect of CNGA2-specific siRNA on adenosine-induced Mn^{2+} influx in H5V cells. A-C: representative traces showing adenosine (100 μmol/L)-induced Mn^{2+} influx in wild-type (A, a responding cell), control siRNA-transfected (B, a responding cell) and CNGA2-specific siRNA-transfected (C, a responding cell) H5V cells. D and E, summary of data showing the effect of CNGA2-specific siRNA on the percentage of cells displaying adenosine-induced Mn^{2+} influx (D), and on the peak Mn^{2+} quenching among the responding cells (E). WT, wild-type; Ctl-si, control siRNA-transfected; CNG-si, CNGA2-siRNA-transfected. Mean ± SEM (n=4-5 independent experiments, 15 to 40 cells per experiment). *P<0.01 as compared to control.

Supplemental figure III

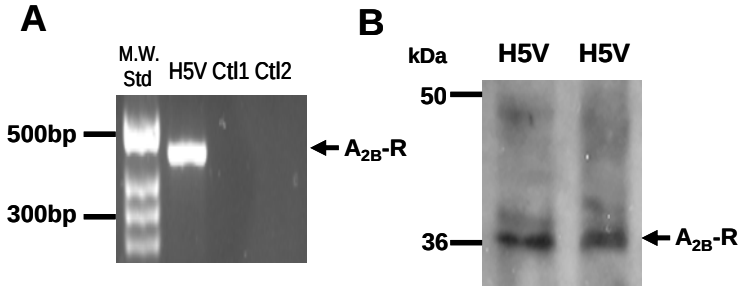

Supplemental figure III. Expression of A_{2B} adenosine receptors in H5V cells. Shown are representative images from RT-PCR (A) and immunoblot (B) from 3-4 independent experiments. A: lane 1, molecular weight standard; lane 2, RT-PCR using total RNA isolated from H5V cells; lane 3, a control in which the procedures were same as in lane 2 except that the step of reverse transcription was omitted; lane 4, a control in which PCR was performed in the absence of cDNA template. B: Immunoblot using an antibody against mouse A_{2B} adenosine receptors. Shown are two identical protein samples isolated from H5V cells.

Supplemental figure IV

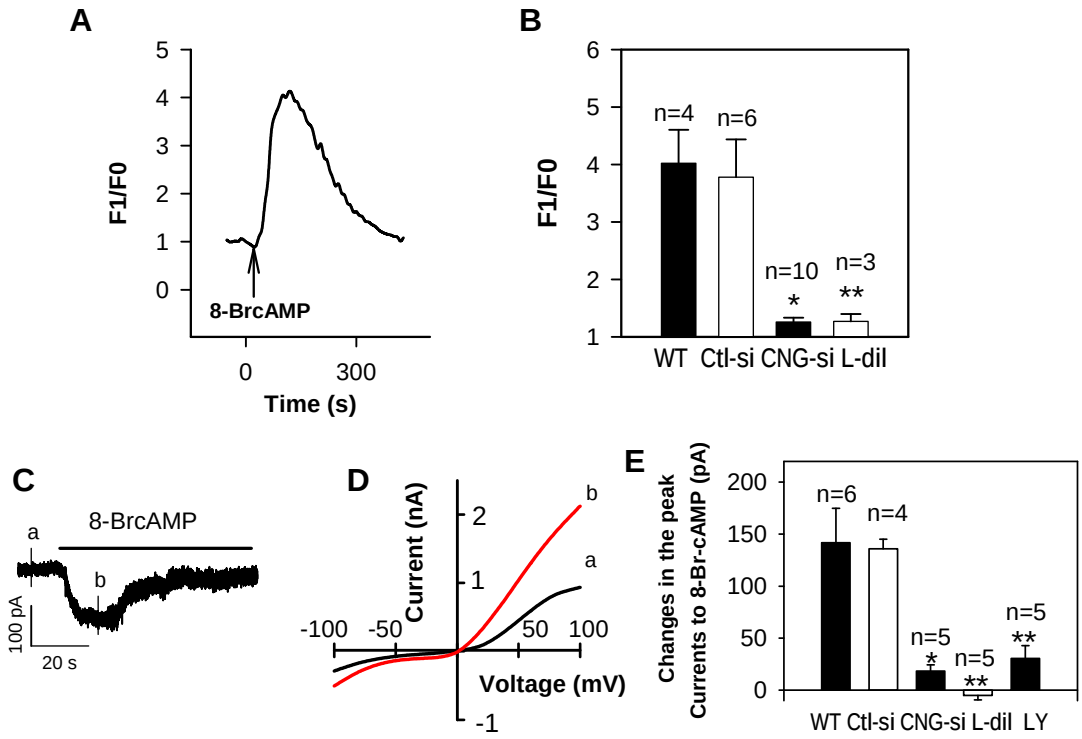

Supplemental figure IV. Effect of the CNGA2-specific siRNA and pharmacological CNGA2 inhibitors on 8-BrcAMP-induced Ca^{2+} influx and cation current in H5V cells. A, a representative trace of 8-BrcAMP (100 μmol/L)-induced $[Ca^{2+}]_i$ rise. B, Summary of data showing the effect of CNGA2-specific siRNA and L-*cis*-diltiazem (50 μmol/L) on the $[Ca^{2+}]_i$ rise. C, a representative trace of 8-BrcAMP (100 μmol/L)-induced inward cation current for a cells clamped at -80 mV. At the time points *a* and *b*, instantaneous *I-V* relationships (D) were obtained by applying an ascending ramp protocol from -100 mV to + 100 mV for 500 ms. E, summary of data showing the effect of CNGA2-specific siRNA, L-*cis*-diltiazem (50 μmol/L), and LY-83583 (20 μmol/L) on 8-BrcAMP-induced peak inward current for cells clamped at -80 mV. WT, wild-type; L-dil, L-*cis*-diltiazem; Ctl-si, control siRNA-transfected; CNG-si, CNGA2-siRNA-transfected. Mean±SE (*n*=3-10 experiments). **P*<0.01 as compared to the control siRNA-transfected H5V cells. ***P*<0.01 as compared to wild-type H5V cells.

Supplemental figure V

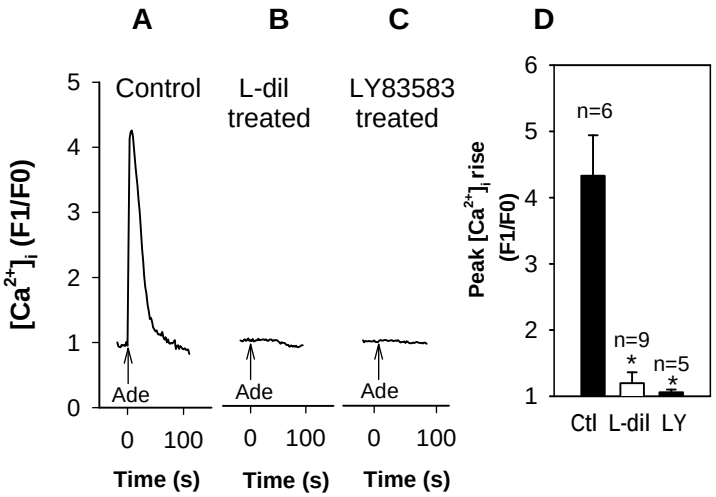

Supplemental figure V. Effect of L-*cis*-diltiazem and LY-83583 on adenosine-induced Ca^{2+} influx in the primary cultured BAECs. A-C, representative traces of adenosine (100 μmol/L)-induced Ca^{2+} influx in control (A), L-*cis*-diltiazem (100 μmol/L)-treated (B) or LY-83583 (20 μmol/L)-treated BAECs (C). D, summary of data showing the effect of chemicals on the peak $[Ca^{2+}]_i$ rise in response to adenosine. Ctl, control; L-dil, L-*cis*-diltiazem; LY, LY-83853. Mean±SEM (*n*=5-9 experiments, 10 to 20 cells per experiment). **P*<0.01 as compared to control BAECs.

Supplemental figure VI

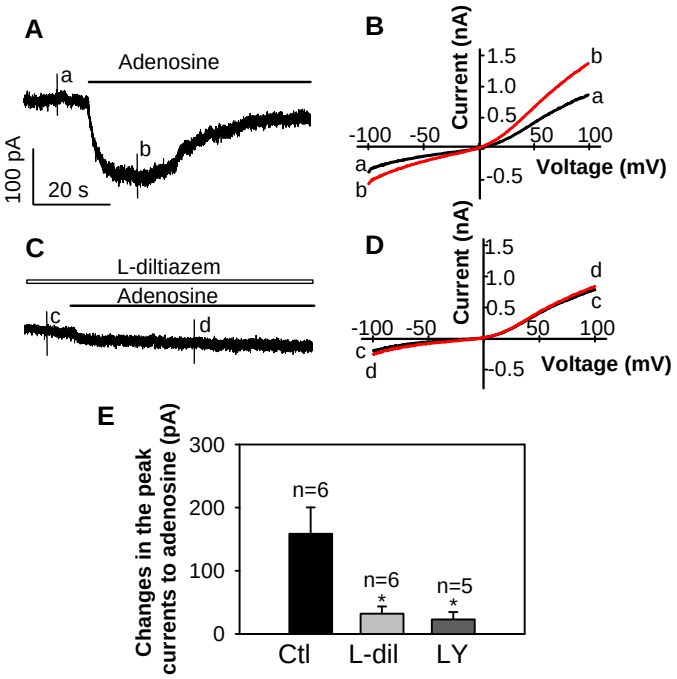

Supplemental figure VI. Effect of L-*cis*-diltiazem and LY-83583 on adenosine-elicited cation current in the primary cultured BAECs. A and C: representative traces of adenosine-stimulated inward current in control (A) and L-*cis*-diltiazem (100 μmol/L)-treated BAEC (C). The cells were clamped at -80 mV. At the time point labeled by *a*-*d*, an ascending ramp protocol was applied from -100 mV to +100 mV for 500 ms to obtain instantaneous *I*-*V* relationships (B, D). E, summary of the data showing the effect of chemicals on adenosine-elicited peak inward current for cells clamped at -80 mV. Mean±SEM (*n*=5-6 patches). **P*<0.01 as compared to control BAECs.

Supplemental figure VII

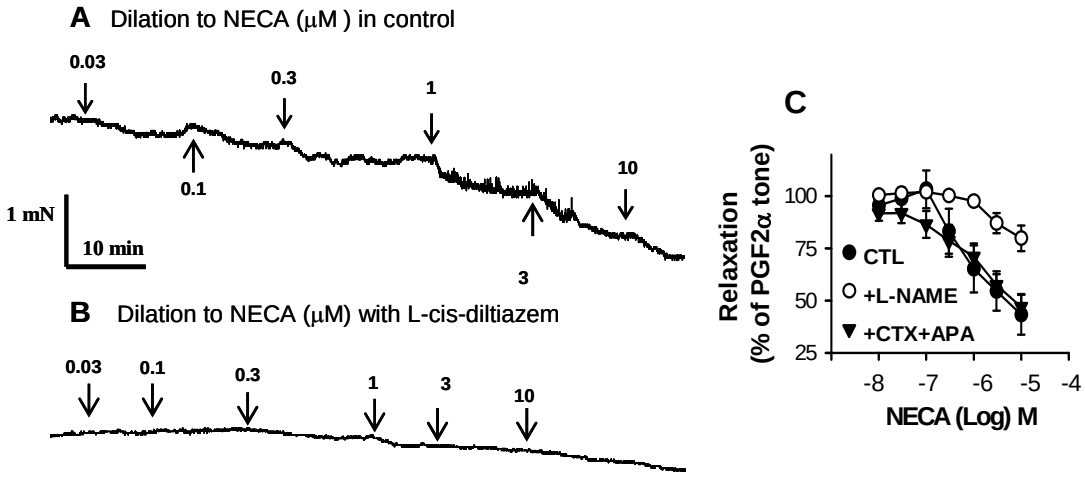

Supplemental figure VII. Effect of L-*cis*-diltiazem, L-NAME, CTX + apamin on NECA-induced vasorelaxation in mouse aortic segments. A and B, representative traces showing the time course of NECA-induced relaxation in mouse aortic segments preconstricted with 11-deoxy prostaglandin $F_{2\alpha}$ in the absence (A) or presence (B) of 100 μmol/L L-*cis*-diltiazem. C, summary of data showing the effect of L-NAME (100 μmol/L) and charybdotoxin+apamin (50 nmol/L each) on NECA-induced relaxation. CTX, charybdotoxin; APA, apamin. All rings were endothelium-intact. Mean±SEM (*n*=5-7). **P*<0.01 as compared to the control.

Supplemental references

Brummelkamp TM, Bernard R, Agami R. A system for stable expression of short interfering RNAs in mammalian cells. *Science* 2002;296:550-553.

Dora KA, Garland CJ, Kwan HY, Yao X. Endothelial cell protein kinase G inhibits release of EDHF through a PKG-sensitive cation channel. *Am J Physiol Heart Circ Physiol.* 2001;280:H1272-H1277.

Garlanda C, Parravicini C, Sironi M, De Rossi M, Wainstock de Calmanovici R, Carozzi F, Bussolino F, Colotta F, Mantovani A, Vecchi A. Progressive growth in immunodeficient mice and host cell recruitment by mouse endothelial cells transformed by polyoma middle-sized T antigen: implications for the pathogenesis of opportunistic vascular tumors. *Proc Natl Acad Sci USA.* 1994;91:7291-7295.

Kleene SJ. Spontaneous gating of olfactory cyclic-nucleotide-gated channels. *J Membr Biol*. 2000;178:49-54.

Kwan HY, Huang Y, Yao X. Regulation of canonical transient receptor potential isoform 3 (TRPC3) channel by protein kinase G. *Proc Natl Acad Sci USA.* 2004;101:2625-2630.

Leung PC, Cheng KT, Liu CL, Cheung WT, Kwan HY, Lau KL, Huang Y, Yao X. Mechanism of noncapacitative Ca^{2+} influx in response to bradykinin in vascular endothelial cells. *J Vasc Res*. 2006;43:367-376.

Yang D, Zhang Y, Nguyen HG, Koupenova M, Chauhan AK, Makitalo M, Jones MR, St Hilaire C, Seldin DC, Toselli P, Lamperti E, Schreiber BM, Gavras H, Wagner DD, Ravid K. The A_{2B} adenosine receptor protects against inflammation and excessive vascular adhesion *J Clin Invest.* 2006;116:1913–1923.